This is the postprint version of: A. Goronovski, R.M. Rivera, T. Van Gerven, A.H. Tkaczyk (2021). Radiological assessment of bauxite residue processing to enable zero-waste valorisation and regulatory compliance. Journal of Cleaner Production 294, 125165.

Radiological assessment of bauxite residue processing to enable zero-waste valorisation and regulatory compliance

Andrei Goronovski[a§], Rodolfo M. Rivera[b,§], Tom Van Gerven[b], Alan H. Tkaczyk[a,c*]

[a] *University of Tartu, Institute of Technology, Ravila 14a, 50411, Tartu, Estonia*
[b] *KU Leuven, Department of Chemical Engineering, Celestijnenlaan 200F, B-3001 Heverlee, Belgium*
[c] *University of Tartu, Institute of Technology, Ravila 14a, 50411 Tartu, Estonia*
[§] *These authors contributed equally to this work.*
[*] *Corresponding author. E-mail address: alan@ut.ee*

Highlights

- Radionuclide concentration after neutralisation is the same as non-neutralised.
- Radionuclide concentration is 150% after separating Fe from the original sample.
- Solid residues can accumulate ^{228}Th above 1000 Bq kg^{-1} after leaching with HCl.
- Analytical model estimates less than 1 mSv/year dose for post-processed BR.

Graphical abstract

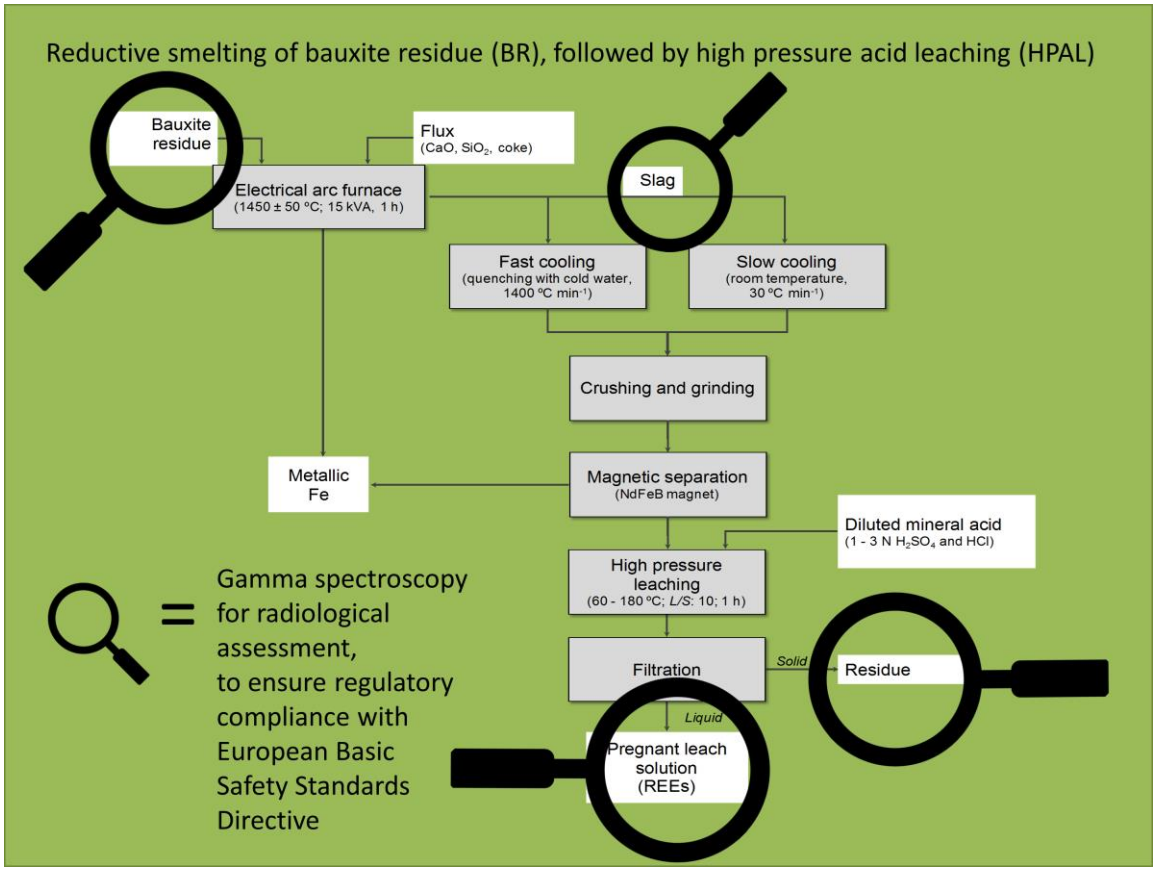

Abstract

In this work, the presence of natural radionuclides in bauxite residue subjected to a neutralisation-leaching process and smelting-leaching process was investigated. The radionuclide concentrations of radium-226, radium-228 and thorium-228 were compared with the concentration of the same radionuclides in the untreated bauxite residue. It was found that neutralisation of bauxite residue at relatively high temperatures (120-150 °C) and high pressure (P_{CO2} = 30 bar) did not change the initial concentration of radionuclides. In fact, the concentration of radionuclides after an intensive neutralisation process remained below 500 Bq kg^{-1}. The separation of iron from the rare-earth elements by reductive smelting permitted a significant decrease of iron concentration in the pregnant leach solution obtained after high pressure acid leaching. However, the radionuclide concentration in the slag was increased 1.5 times with respect to the initial concentration, although it did not exceed 800 Bq kg^{-1}. Further processing of the slags by high pressure acid leaching led to the dissolution of several base metals, while a portion of the radionuclides remained unreacted in the solid fraction. Thus, a concentration of thorium-228 > 1000 Bq kg^{-1} was only observed after leaching a calcium oxide-based slag with hydrochloric acid. Meanwhile, in the leach liquors, the concentration of radionuclides was < 100 Bq L^{-1}. Nevertheless, based on analytical estimations using conservative assumptions, the solid residues and leach liquors produced by acid leaching in the current study are unlikely to exceed the exposure limit of 1 mSv set by the European Basic Safety Standards Directive. It should be noted that the current results are based on a specific bauxite residue studied in this work, and caution should be used in the application to other situations. The described radiological assessment of bauxite residue processing can ensure the necessary regulatory compliance and facilitate zero-waste valorisation.

Keywords:

Radiological assessment, environmental radioactivity, regulatory compliance, waste processing, high pressure acid leaching (HPAL), iron smelting

Table of abbreviations

BR – bauxite residue

BSS – Basic Safety Standard

EAEC (or Euratom) - European Atomic Energy Community

FC – fast cooling

HPAL – high pressure acidic leaching

MDA – minimum detectable activity

PLS – pregnant leach solution

REEs – rare-earth elements

SC – slow cooling

1 Introduction

Bauxite residue (BR, also known as red mud) is a by-product generated during the production of alumina from bauxite ore by the Bayer process. BR is composed of compounds that are insoluble in concentrated NaOH solutions such as Fe- and Ti-rich minerals, undigested Al-rich minerals, Na/Al-hydro-silicates, and Ca compounds. Rare-earth elements (REEs) can also be present in BR at non-negligible concentrations. For temporary or long-term storage, BR undergoes filter-pressing, where it is dewatered for dry landfilling.

Presently, only a minor portion of BR is industrially reused (Evans, 2016). Due to the large quantity of BR produced each year (ca. 150 million tonnes) and the accumulation in large deposits, there is significant interest from the industrial sector to economically utilise BR, either by recovery of valuable metals or by use in bulk applications (International Aluminium Institute, 2015). Besides the concentration of valuable metals, BR can also contain some levels of naturally occurring radionuclides, whose concentration mainly depends on the origin of the bauxite ore (Cooper, 2005; Cuccia et al., 2011; Goronovski et al., 2019). From these, ^{40}K, ^{238}U, ^{232}Th and their decay products are

the most important ones (Evans, 2016). In nature, Th and U tend to occur in similar mineral phases as do the REEs (Gupta and Krishnamurthy, 2005).

Furthermore, it is possible to link the observed radionuclides to specific minerals. Within bauxites, radionuclides can appear as part of the radionuclide-rich minerals monazite and ilmenite (IAEA, 2003). The association of Th with Ti-rich mineral phases has been previously reported in bauxite minerals from Greece (Gamaletsos et al., 2011). During the Bayer process, U tends to dissolve but subsequently re-precipitates, ending up associated with the coarser BR fraction (Barakos et al., 2014). Within BR, Th can be associated with rare-earth ferro-titanate compounds (REE,Ca,Na)(Ti,Fe)O_3 (Vind et al., 2018) and the newly derived (nano-)perovskite ($CaTiO_3$) mineral (Gamaletsos et al., 2016a).

1.1 Radionuclide concentration in different bauxite residues

The European Basic Safety Standards Directive (EU BSS) (European Parliament, 2014) states that legislation of European countries must account natural radionuclides to the same extent as artificial. This means that for both natural and artificial radionuclides, the same limit on effective dose (i.e. 1 mSv per year for the members of the public) must apply. An important relevant concept is the exemption limit, which defines the concentration below which it is possible to exempt a radionuclide from radiological regulatory control. The EU BSS sets the following exemption limits for naturally occurring radionuclides: 1000 Bq kg^{-1} in the case of ^{238}U, ^{232}Th and their daughter nuclides (individually), and 10000 Bq kg^{-1} in the case of ^{40}K. Comparison with the exemption limits provided by the EU BSS can be used to determine if industrial practices could realistically result in members of the public exceeding the permitted effective dose (i.e., 1 mSv per year). Concentrations below the exemption limit imply that the specific material does not pose a threat to humans. If the material in question have radionuclide content in excess of the exemption limits, this does not necessarily imply that the material poses a threat to humans, but indicates that the material should be subjected to further assessment.

The reported concentration of natural radionuclides in BR produced in different countries is shown in Table 1. According to the limits set by the European Atomic Energy Community (EAEC or Euratom) and the concentrations shown in Table 1, Th is only present in significant levels in BR from Australia. On the contrary, BRs produced in Europe can be considered unlikely to cause elevated exposure to ionizing radiation due to low radionuclide content and, they can often be exempted from radiological regulatory control. Still, it should be noted that BR's radiological properties can be modified when BR is further processed to recover valuable metals (e.g., Al, Fe, Ti and REEs). For instance, as it was reported by Hegedűs et al., after leaching about 85% of Th and Po (including ^{210}Po, a decay product of ^{238}U) can remain in the solid residue with a radioactivity < 370 Bq kg^{-1} (Hegedűs et al., 2018). In a different study, the radiological properties of post-processed BRs by sintering, smelting and acid leaching (for the recovery of Al, Fe and REE, respectively) were also examined; the sintered and the leached sample reported a concentration of radionuclides < 700 Bq kg^{-1}, while the slag from the smelting process demonstrated a possibility of having concentration higher than 1000 Bq kg^{-1} (Goronovski and Tkaczyk, 2019). Samouhos et al. also reported a substantial radionuclide enrichment when Fe was separated from the BR by reductive roasting (Samouhos et al., 2013). Notice that the separation of Fe from BR is essential to ensure the technological feasibility and economic viability of an integrated process capable to recover REEs (Narayanan et al., 2018).

Table 1: Natural radioactivity (Bq kg^{-1}) of bauxite residue produced in different countries.

Country	^{238}U	^{232}Th	^{40}K	Reference
Greece	170 ± 2	404 ± 15	26 ± 8	(Goronovski and Tkaczyk, 2019)
Spain	203 ± 35	598 ± 18	62 ± 13	(Rubinos and Barral, 2013)
China	350 ± 21	414 ± 41	583 ± 18	(Gu et al., 2017)
Turkey	210 ± 6	539 ± 18	112 ± 7	(Akinci and Artir, 2008)
Australia	310 ± 20	1350 ± 40	350 ± 20	(Nuccetelli et al., 2015)
Brazil	139 ± 1	350 ± 19	45 ± 2	(Cuccia et al., 2011)
Germany	122	183	N.d.	(Nuccetelli et al., 2015)
Hungary	299 ± 49	314 ± 75	48	(Nuccetelli et al., 2015; Somlai et al., 2008)
Jamaica	709 ± 479	339 ± 16	300 ± 49	(Pontikes and Angelopoulos, 2013)

n.d.: not determined

At present, there is no systematic study on the radionuclide concentration in solid or liquid streams produced during the integration of smelting and acid leaching. Such knowledge requires a comprehensive study of radionuclide concentrations within the process, with the aim to predict their behaviour starting from untreated BR until the production of solid residues and leachates liquors produced after acid leaching.

1.2 Metal separation from bauxite residue in view of rare-earth elements recovery

During conventional (direct) acid leaching of BR, the increase in dissolution of rare-earth elements (REEs) is associated with a high consumption of mineral acid and a substantial co-dissolution of Fe, which leads to low efficiencies in downstream processing (i.e., solvent extraction or ion exchange). Neutralisation of BR with CO_2 was reported as a potential technology for reducing acid consumption in the acid leaching step for metal recovery from BR. Although neutralisation of BR with CO2 gas did not enhance the extraction of REEs during acid leaching, it did help to reduce the alkalinity (Rivera et al., 2017a). The co-dissolution of Fe is detrimental, as it is difficult to separate it from REEs and Sc in particular, requiring a large quantity of reagents during downstream processing. Sc tend to be chemically associated with the Fe(III)-rich oxide lattice, which limits its complete dissolution (Borra et al., 2015; Rivera et al., 2017a). Therefore, Fe must be removed in advance in order to improve the extraction and selectivity of REEs.

Smelting of BR leads to the reduction of iron oxides to produce a REE-rich slag and pig iron (i.e., a metallic product generated from a smelting furnace with an Fe content usually above 90 wt%). The REE-rich slag can be chemically separated by acid leaching. However, in conventional acid leaching, silica gel can form due to the dissolution of silicate minerals, which significantly affects the filtration efficiency of the leach liquor. Due to the high concentration of silica in the slag (as a consequence of adding SiO_2 as flux), room temperature acid leaching can no longer be considered because of silica polymerization (or silica gel formation). A method which avoids silica-associated problems is high pressure acid leaching (HPAL), i.e. acid leaching performed at high temperature in an autoclave.

HPAL also helps deplete other major metals such as Ti, due to its hydrolysis at high temperature. The integration of reductive smelting with HPAL was previously reported as an innovative process technology to selectively recover REEs from BR (Rivera et al., 2019b).

From an economic perspective, it can be noted that solely recovering Fe (among others base metals) from BR may not ensure the economic viability of BR processing. However, profit margins for BR processing can be significantly improved via approaches which combine recovery of Fe alongside REEs and Sc in particular (Borra et al., 2016).

In the current work, the presence of natural radionuclides in BR subjected to a neutralisation-leaching process, BR slags arising from the smelting of BR, and the leachates and solid residues obtained from HPAL process, were investigated. Thus, the radionuclide concentration of ^{226}Ra (decay product of ^{238}U), ^{228}Ra and ^{228}Th (decay products of ^{232}Th), were compared with the concentration of the same radionuclides in the untreated BR. ^{40}K initially exists in BR in small amounts, and in the current study, it remained below Minimum Detectable Activity (MDA) in all the studied secondary residues and leachate samples. The MDA values for this isotope are summarised in the Supplementary Material section.

2 Materials and methods

BR used in the current work was received from the alumina refinery after dewatering by filter pressing and drying at ambient temperature. Upon arrival in the laboratory, the sample was further dried at 105 °C for 24 h. The sample was further processed via reductive smelting by considering different mixture of fluxes. The smelting reduction experiments were carried out in an electrical arc furnace (100 kVA direct current) at a temperature of 1500 ± 50 °C during 1 h. After heating, the molten material was cooled down at two different cooling rates: (1) quenching with cold water (pouring the slag in water at room temperature, cooling rate about 1400 °C min^{-1}, fast cooling) and (2) room temperature cooling by keeping the slag in the crucible (cooling rate about 30 °C min^{-1}, slow cooling). The Fe-metal fraction produced in the smelting experiment was separated from the slag and

kept for further analysis. The slag was crushed into small pieces (< 2 cm) with a hammer and was subsequently crushed in a laboratory jaw crusher (Retsch BB 51) to produce material 100% finer than 1 mm.

Conventional acidic leaching of BR and BR slags at room temperatures can result in the formation of polymerized silica gel, which resulted difficult to filtrate and, consequently, affects the efficient separation of REE (Rivera et al., 2017). To tackle this issue, (HPAL) was considered instead. The slags were processed by HPAL in a titanium autoclave (Parr Company, series 4560, 400 mL capacity) varying the temperature between 60-180 °C. H_2SO_4（95–97 wt%, Sigma–Aldrich) and HCl (37 wt%, Fisher Scientific) were studied as leaching reagents. The leaching experiments were performed with a liquid-to-solid ratio, *L/S*, of 10:1 to ensure a substantial leaching concentration of REEs in the leach liquor with a reasonable consumption of bauxite residue. The procedure, chemical and mineralogical analyses of the slags and recovery rates of metals, as well as the results of the HPAL of slags arising from the smelting of BR, have been reported elsewhere (Rivera et al., 2019b).

Gamma-ray spectroscopy method was applied to quantify radionuclide content in the BR slags generated after reductive smelting, and the solid residue and leachates produced after HPAL. The amount of every solid sample was in the order of 1-3 g. To ensure homogeneous mixture and constant solid geometry, they were mixed with ca. 5 g of epoxy resin in Al-based containers, which after the sample was solidified, were tightly sealed to avoid any leakage of Rn. Liquid samples were dried under infrared lamps for 6-12 h. The resulting solid mass was then ground to produce a homogeneous powder, which was processed in the same way as the solid samples. Once the samples were prepared, they were kept intact for approximately 4 weeks for ^{226}Ra, and its decay products, to reach secular equilibrium. In the current work ^{238}U and ^{232}Th were not measured directly, instead their daughter nuclides were studied. The activity concentration of ^{226}Ra, ^{228}Ra and ^{228}Th was determined based on their daughter nuclides ^{214}Pb, ^{228}Ac and ^{212}Pb respectively, and ^{40}K was measured directly. The gamma lines used for measurements are summarized in the Table . Two high purity Ge-based detectors were used: GEM- 35200 (EG&G Ortec) coaxial detector and BE3830P (Canberra).

Table 2: Isotopes with their corresponding gamma lines (in keV) considered in this research. Isotopes in brackets corresponded to the daughter nuclides that were measured.

Isotope	**Gamma lines (keV)**		
^{40}K		1460.82	
^{226}Ra (^{214}Pb)	242.00	295.22	351.93
^{228}Ra (^{228}Ac)	338.32	911.20	968.96
^{228}Th (^{212}Pb)		238.63	

The samples were prepared in exactly the same way as the calibration standards produced from certified IAEA natural U and Th reference materials (IAEA, 2010). The differences in the material matrixes and coincidence summing corrections have been addressed with the help of EFFTRAN model (Vidmar, 2005).

2.1 Radiological exposure assessment

For solid samples that exceed EU BSS concentration limits and liquid samples, it is important to demonstrate that they are safe to handle and would not exceed the regulatory exposure limit for workers or the general public. A straightforward theoretical model has been applied to demonstrate maximum theoretical exposure coming from the developed materials. An infinitely large residue stockpile with infinite depth was assumed. The exposure to gamma radiation for a worker wearing personal protective equipment, but without radiation shielding, for a period of 1000 hours annually, was also considered. Such a stockpile would provide a similar exposure to that coming from radionuclides present in soil. In the research conducted by Markkanen, comparable sets of dose conversion factors were derived for exposures coming from an infinite material stockpile and soil (Markkanen, 1995). These coefficients are similar to those recommended by UNSCEAR for terrestrial radionuclides present in soil (UNSCEAR, 2000). The latter were applied in the current study, and the Equation 1 was used to estimate annual exposure to a person working on a residue pile with known concentration [ibid.].

$$Dose = \sum(C_a \cdot DC_a) \cdot T \cdot F \qquad (1)$$

Where:

C_a is the isotope *a* concentration (Bq kg^{-1});

DC_a is the dose coefficient for isotope *a* decay chain, summarized in Table (nGy h^{-1} per Bq kg^{-1});

T is the exposure time (h y^{-1});

F is the dose rate conversion factor (Sv/Gy), equals to 0.7 (UNSCEAR, 2000).

Table 3: Dose coefficients for ^{40}K and undistorted ^{238}U and ^{232}Th decay chains for soil (UNSCEAR, 2000) and infinite material stockpile (Markkanen, 1995).

Radionuclide series	**Dose coefficient (nGy h^{-1} per Bq kg^{-1})**	
	Soil	**Infinite stockpile**
^{40}K	0.0417	0.042
^{238}U	0.462	0.470
^{232}Th	0.604	0.570

For liquid samples, the volumetric concentrations were converted into mass concentration by using the density of the corresponding mineral acids used in this research, i.e. HCl (1.2 g cm^{-3}) and H_2SO_4 (1.84 g cm^{-3}).

In the current study, ^{238}U and ^{232}Th were not measured directly, instead ^{226}Ra represents the decay chain of U. It should be noticed that ^{226}Ra and its decay products provide a major contribution to the gamma dose coming from the ^{238}U decay chain and this isotope is used as a proxy for ^{238}U to model gamma exposure (European Commission, 1999). The highest concentration of either ^{228}Ra or ^{228}Th was used to represent the whole decay chain of ^{232}Th. However, during post-processing of BR, ^{232}Th decay chain can be disrupted leading to a different behaviour of radionuclides. Hence, for the sake of conservatism, the highest measured nuclide concentration was selected, and a non-disturbed decay chain was assumed in the model.

3 Results and discussion

3.1 Chemical composition of bauxite residue

The BR used in the current work was provided by Mytilineos S.A. - Aluminium of Greece (Agios Nikolaos, Greece). It was generated predominantly from Greek (karst) bauxite ore. It originates from a mixture of 80 wt% karst and 20 wt% lateritic bauxites. Chemical composition, as well as a typical range composition are summarized in the Table .

Table 4: Chemical composition of currently studied bauxite residue and typical composition ranges.

Component	Current composition [wt%] (Rivera et al. 2017)	Typical composition [wt%] (Evans, 2016)
Fe_2O_3	46.7	5 – 60
Al_2O_3	18.1	5 – 30
SiO_2	7.3	3 – 50
TiO_2	5.8	0.3 – 15
CaO	8.5	2 – 14
Na_2O	2.8	1 – 10

Previous studies have demonstrated that radionuclides are enriched in this BR by a factor of about 1.7-2.3 (Goronovski et al., 2019) compared to the initial bauxites. Particularly, in this BR, Th has been reported to be associated with Ti-rich perovskite-type mineral phases (Gamaletsos et al., 2011).

3.2 Radionuclide concentration in neutralised and neutralised-leached bauxite residue

The neutralisation of BR with CO_2 was reported as an alternative process to reduce the acid consumption in the subsequent acid leaching step (Rivera et al., 2017). The pH of the BR was reduced < 9.0 when neutralisation was performed with a CO_2-partial pressure (P_{CO2}) of 30 bar and temperatures > 60 ºC during 2 h of experiment. Neutralisation of BR with CO_2 did not cause a significant change in the concentration of base (e.g., Al, Fe, Ti) and trace elements (e.g., rare-earth elements, REEs) (Rivera et al., 2019a). In fact, the concentration of metals was observed to remain the same as in the untreated BR. Figure 1 shows the radionuclide concentration in samples of BR and in BR subjected to neutralisation at 120 and 150 ºC (P_{CO2} = 30 bar). Correspondingly, the radionuclide

concentration in samples of BR subjected to neutralisation conditions remained unchanged as in the untreated BR, i.e. < 500 Bq kg^{-1}. The same phenomenon was reported early on the distribution of REEs in non- and neutralised BR (Rivera et al., 2019a). The relatively low radionuclide concentration allows the safe disposal of this material with or without neutralisation.

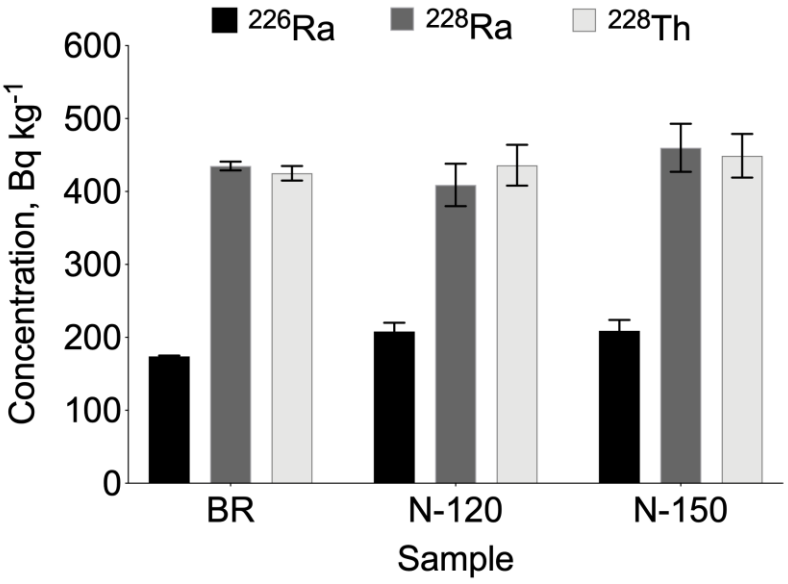

Figure 1: Radionuclide concentration (in Bq kg^{-1}) in the bauxite residue (BR), in BR subjected to neutralisation at 120 ºC (N-120) and 150 ºC (N-150). Neutralization was performed with a CO_2-partial pressure (P_{CO2}) of 30 bar.

3.3 Reductive smelting followed by high pressure acidic leaching

The flow sheet for reductive smelting of BR, followed by HPAL of the slag arising during the smelting process is presented in Figure 2 (Rivera et al., 2019b). The separation of Fe from the REEs by reductive smelting, allowed to significantly decrease the concentration of Fe in the pregnant leach solution (PLS) obtained after leaching, as it can be seen in Figure 3. The extraction of Al from the slag, however, was very high (14-17 g L^{-1}) with both mineral acids. Due to the enrichment of Al in the slags, its concentration in the leach solution was 3-4 times higher than the concentration obtained after processing the BR directly. The concentration of Si was lower than 1 g L^{-1}, which allowed to avoid the formation of silica gel (Rivera et al., 2017). Ti was scarcely dissolved and, consequently, its concentration in the leach solution was also low (< 0.3 g L^{-1}), remaining in the solid residue

associated to O and/or Ca in the mineral phases anatase/rutile (TiO_2) and/or perovskite ($CaTiO_2$), although perovskite was identified in the solid residue that remained from HPAL with HCl only.

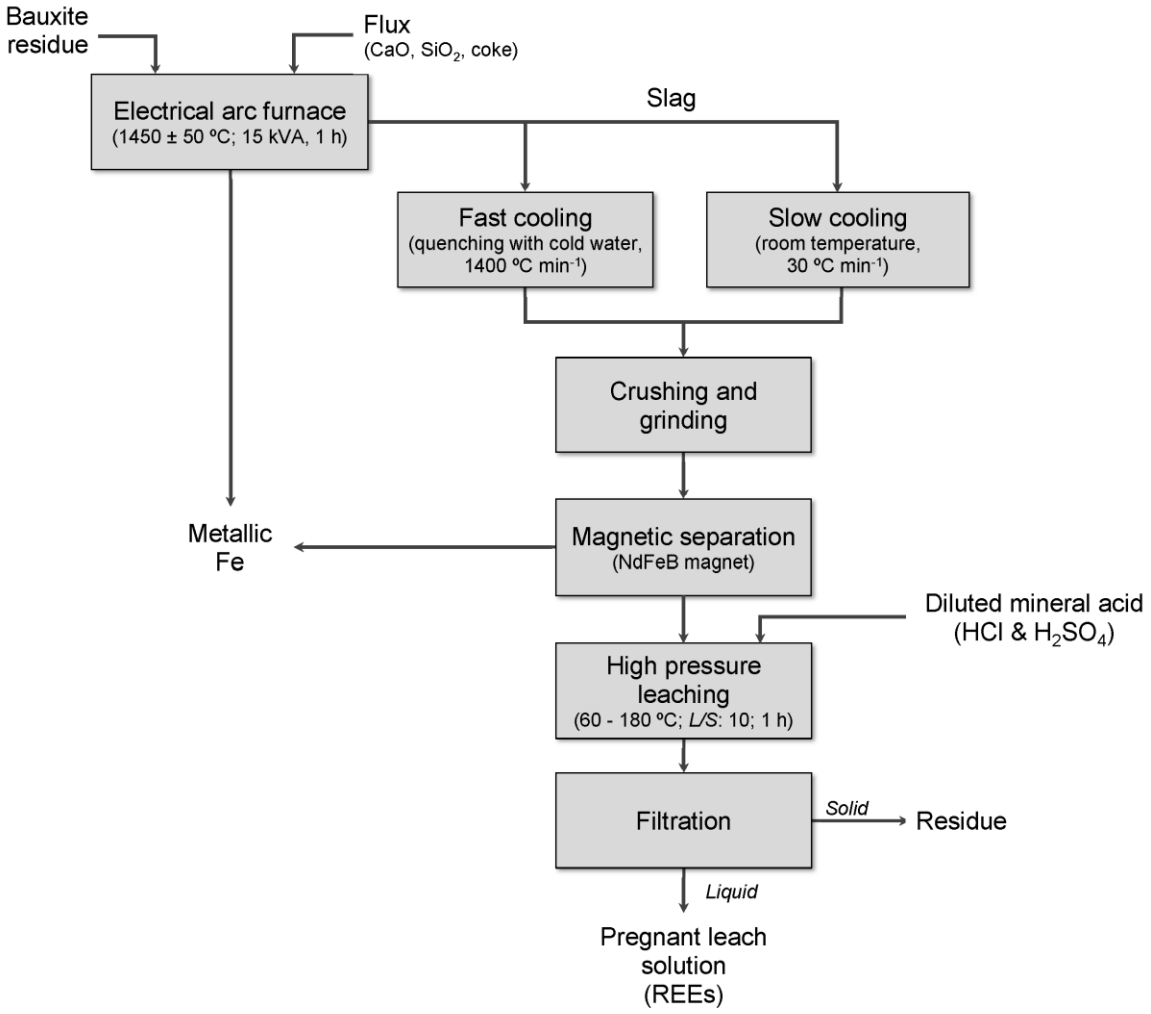

Figure 2: Flow sheet for reductive smelting of bauxite residue, followed by high pressure acidic leaching of the slag arising during the smelting process (reprinted from (Rivera et al., 2019b) with permission of Elsevier; license number: 4700150872449).

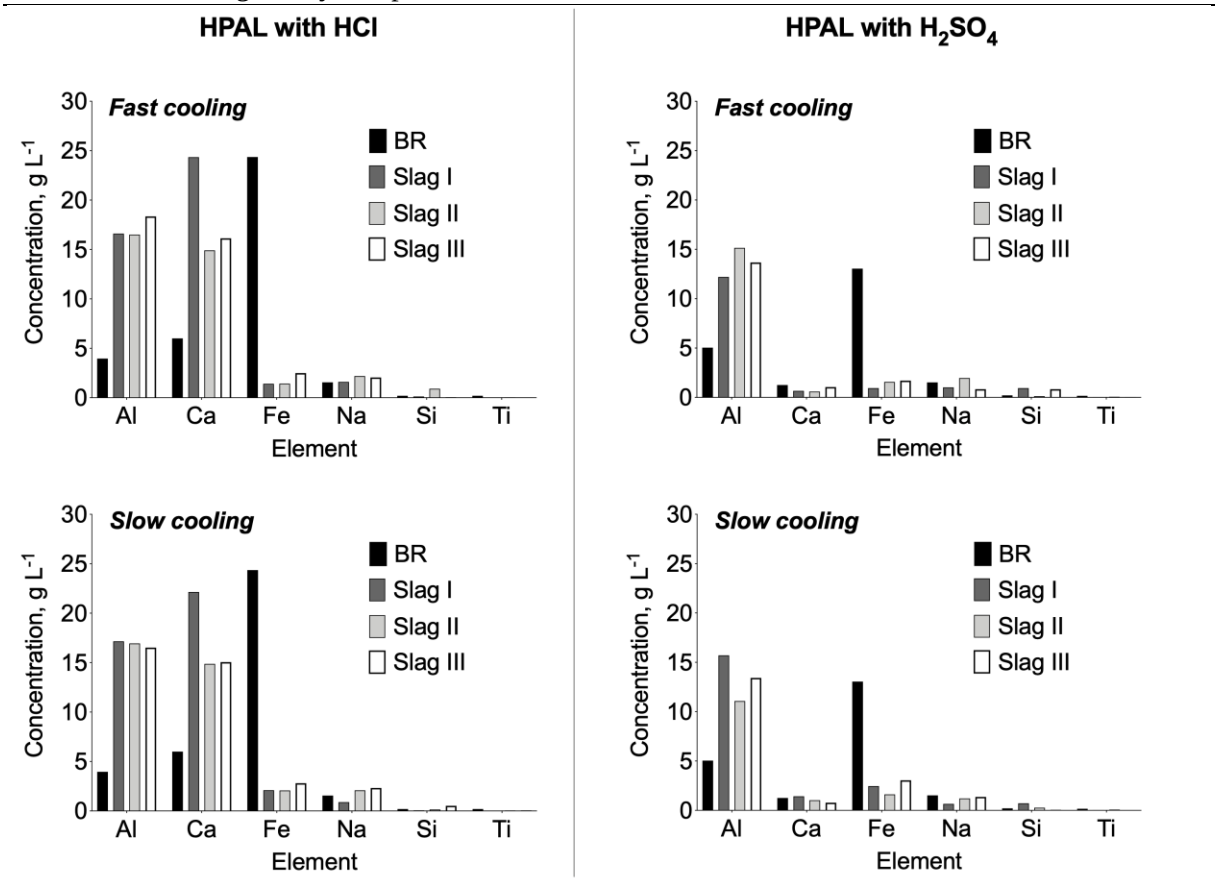

Figure 3: Concentration (in g L^{-1}) of major metals (Al, Ca, Fe, Na, Si and Ti) after high pressure acidic leaching (HPAL) with diluted HCl (at 120 ºC, 3 mol L^{-1}) and H_2SO_4 (at 150 ºC, 1.5 mol L^{-1}) of bauxite residue (BR) and bauxite residue slags (*L/S*: 10, *t*: 1 h).

3.3.1 Radionuclide concentration in bauxite residue slags

The radionuclide content of the untreated BR, and the BR slags produced after the smelting process is presented in Figure 4. As it was expected, the mere separation of Fe from BR by smelting led to a high enrichment of radionuclides in the slags. This resulted in an average accumulation ratio of about 1.5 with respect to the radionuclide content in the untreated BR. The radionuclides measured in these slags behaved in the same way and had similar accumulation ratios.

The concentration of ^{40}K was below MDA, i.e. < 300 Bq kg^{-1}, in all the BR slag samples (see the Supplementary Material section). The radionuclides ^{228}Ra and ^{228}Th did not exceed a concentration of 800 Bq kg^{-1} and, therefore, they were below exemption level from regulatory control criteria set as 1000 Bq kg^{-1} for ^{238}U (decay products ^{226}Ra, ^{214}Pb) and ^{232}Th (and their decay products). Although in

this research the radionuclide content in the metallic Fe produced after smelting was not measured, the presence of trace amounts of radionuclides can also be expected as a part of impurities that can reach 3-5% in the pig iron.

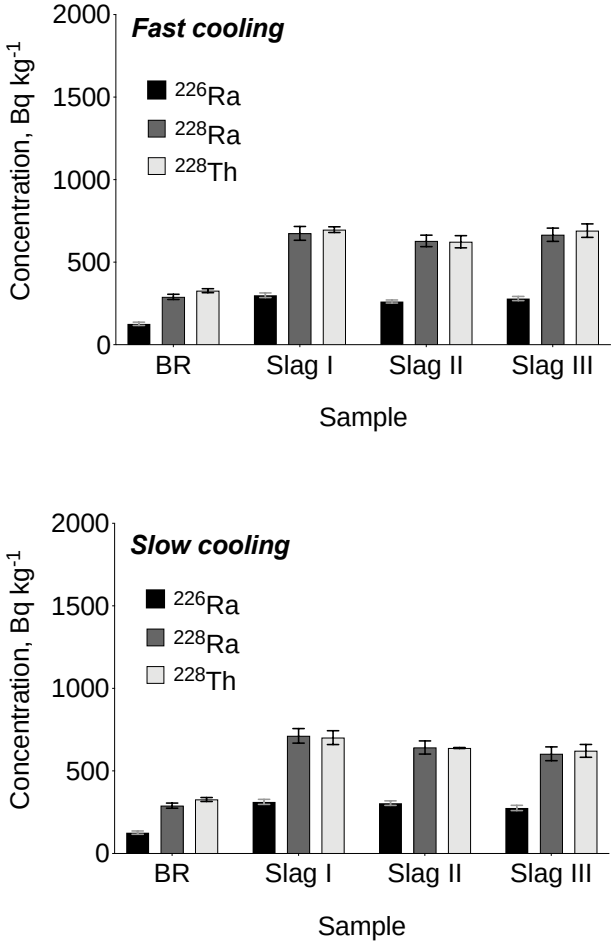

Figure 4: Radionuclide concentration (in Bq kg^{-1}) in bauxite residue (BR) and bauxite residue slag samples.

3.3.2 Radionuclide concentration in solid residues and leach liquors obtained after high pressure acidic leaching

Figure 5 shows the radionuclide content of the solid residues that remained after HPAL of BR slags with diluted HCl (at 120 ºC, 3 mol L^{-1}) and H_2SO_4 (at 150 ºC, 1.5 mol L^{-1}) (*L/S* = 10, 120 ºC, t: 1 h). It should be noted that some of the samples were not available for gamma-ray spectrometry as they were

consumed in other analysis. In the figures, these samples are marked as "not determined". In the solid residues remaining after HPAL (Figure 5), differences in (i) behaviour of specific radionuclides as well as (ii) influence of experimental conditions on the accumulation of radionuclides, were observed. Still, except for the solid residue generated from slag I, the radionuclide content remained < 1000 Bq kg^{-1} after leaching.

Slag I was produced by mixing BR with 20 wt% of CaO as flux and 10 wt% of lignite coke. Meanwhile, in slag II and III, only 8-10 wt% of CaO was utilised as flux, which was mixed with 10-15 wt% SiO_2. In the slags, Ca was found associated to different Al/Si/O- and Al/Na/O-mineral phases, but also associated to Ti, as in the perovskite ($CaTiO_3$) mineral phase (Rivera et al., 2019b). Slag I, which was produced with the highest content of CaO as flux, was mainly characterised by the presence of gehlenite ($Al_2Ca_2SiO_7$) and perovskite (CaO_3Ti). The presence of such mineral phases was less significant in the other slags due to the low Ca content. During acid leaching, Ca-rich mineral phases were less soluble with H_2SO_4 than with HCl due to the tendency to form $CaSO_4$, which encloses partial or totally Ti/O-phases (Rivera et al., 2019b). On the other hand, acid leaching with HCl led to a high dissolution of most of the elements. However, in the presence of both two mineral acids, the co-dissolution of Si and Ti was suppressed during high pressure leaching. As it has been reported, Th can be chemically attached to Ti-mineral phases, as both elements share the same tetravalent oxidation state (Gamaletsos et al., 2016b); thus, Th can also remain in the solid fraction after leaching. Hence, the content of the isotope ^{228}Th was the highest in the solid residue obtained from leaching slag I, due to the enrichment of Ti-phase by the high dissolution of Ca and Al, when HCl was used as the leaching reagent (see Figure 3).

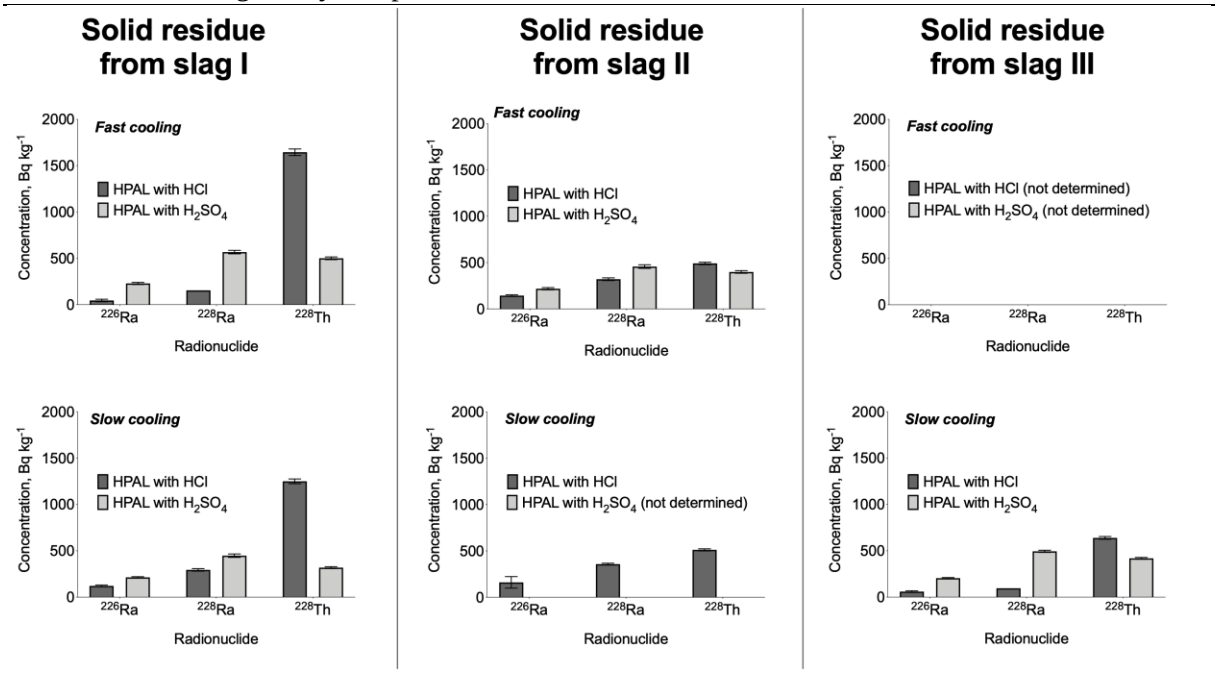

Figure 5: Radionuclide concentration (in Bq kg^{-1}) in solid residues generated after high pressure acidic leaching of bauxite residue slag samples with HCl (at 120 ºC, 3 mol L^{-1}) and H_2SO_4 (at 150 ºC, 1.5 mol L^{-1}). Leaching conditions: *L/S* = 10, t: 1 h.

As depicted in Figure 6, a non-negligible concentration of radionuclides was also detected in the corresponding leach liquors obtained after HPAL. Noticeable was the relatively high concentration (ca. 80 Bq L^{-1}) depicted by ^{226}Ra and ^{228}Ra when the slags II (subjected to slow cooling) and III (subjected to fast cooling) were leached with HCl. However, with H_2SO_4 as a leaching reagent, the concentration of ^{226}Ra, ^{228}Ra and ^{228}Th resulted in values lower than 40 Bq L^{-1}. Still, a further enrichment can be expected with subsequent separation processes, namely solvent extraction or ion exchange. It should be noted that the half-lives of ^{226}Ra, ^{228}Ra and ^{228}Th isotopes are 1600, 5.8 and 1.9 years respectively, which must be taken into consideration for further processing.

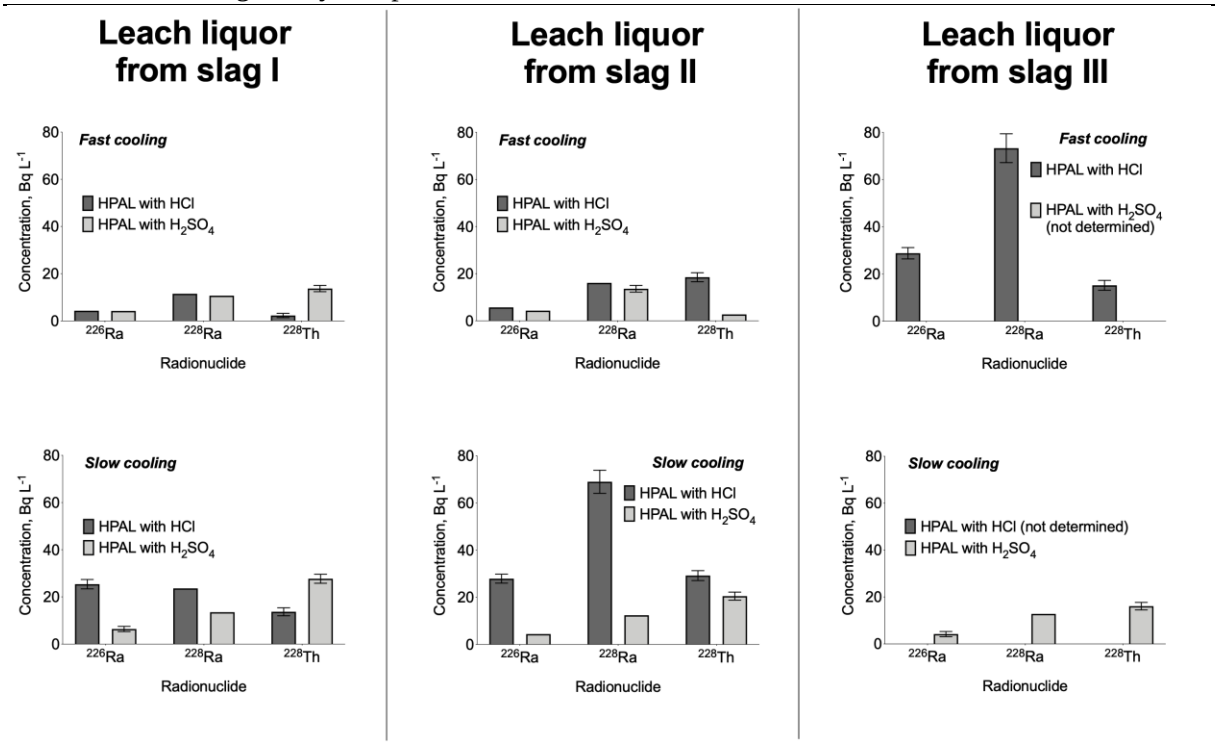

Figure 6: Radionuclide concentration (in Bq kg^{-1}) in leach liquors generated after high pressure acidic leaching of bauxite residue slag samples with HCl (at 120 ºC, 3 mol L^{-1}) and H_2SO_4 (at 150 ºC, 1.5 mol L^{-1}). Leaching conditions: *L/S* = 10, t: 1 h.

3.3.3 Radiological implications

Some of the samples studied in the current work exceeded the exemption limits set in the EU BSS for the content of ^{228}Th. As stated previously, these findings do not confirm that these materials would jeopardize the public safety, if they are handled on an industrial scale. However, an additional evaluation of these selected samples could be necessary to ensure compliance with radiological regulations. In order to demonstrate the maximum potential exposure coming from the accumulated radionuclides, a conservative approach has been selected to model potential exposure to workers, assuming infinitely large stockpiles of the materials (see Section 2.1 for further details). Table 2-7 summarise the resulting doses which could be obtained, considering highly conservative assumptions.

Table 2: Post-processed bauxite residue samples and corresponding modelled annual dose (N-120 and N-150: bauxite residue subjected to neutralisation at 120 and 150 °C, respectively; Lx-NBR-0.5N and Lx-NBR-1.6N: leached-neutralised bauxite residue with 0.5 N and 1.6 N H_2SO_4, respectively; FC and SC: slags subjected to fast and slow cooling, respectively).

Sample	Dose (mSv)
N – 120	0.26
N – 150	0.27
Lx – NBR – 0.5N	0.29
Lx – NBR – 1.6N	0.45
Slag I – FC	0.39
Slag II – FC	0.35
Slag III – FC	0.39
Slag I – SC	0.40
Slag II – SC	0.38
Slag III – SC	0.36

Table 3: Maximum theoretical annual doses from solid residues and leach liquors produced after high pressure acidic leaching with HCl. In case radionuclide concentration was not measured, the minimum detectable activity value was used instead.

Sample	Dose (mSv)	
	Solid sample	Liquid sample
Slag I – FC	< 0.73	$< 6.5 \cdot 10^{-3}$
Slag I – SC	< 0.58	$< 1.7 \cdot 10^{-2}$
Slag II – FC	< 0.26	$< 9.6 \cdot 10^{-3}$
Slag II – SC	< 0.27	$< 3.3 \cdot 10^{-2}$
Slag III – FC	N.d.	$< 3.6 \cdot 10^{-2}$
Slag III – SC	< 0.30	N.d.
HPAL – BR	< 0.19	$< 1.8 \cdot 10^{-2}$

n.d.: not determined

Table 4: Maximum theoretical annual doses from solid residues and leach liquors produced after high pressure acidic leaching with H_2SO_4. In case radionuclide concentration was not measured, the minimum detectable activity value was used instead.

Sample	Dose (mSv)	
	Solid sample	Liquid sample
Slag I -FC	< 0.30	$< 4.7 \cdot 10^{-3}$
Slag I-SC	< 0.22	$< 8.4 \cdot 10^{-3}$
Slag II-FC	< 0.25	$< 4.7 \cdot 10^{-3}$
Slag II-SC	N.d.	$< 6.3 \cdot 10^{-3}$
Slag III-SC	< 0.25	$< 5.4 \cdot 10^{-3}$
BR	< 0.16	$< 6.1 \cdot 10^{-3}$

n.d.: not determined

These results demonstrate that the studied materials, under the specific experimental conditions considered in this research, are unlikely to exceed regulatory dose limits due to gamma ray exposure even if stored in an infinitely large material stockpile.

4. Conclusions and future prospects

Bauxite residue represents an interesting source for critical metals which can be recovered by hydro- and/or pyrometallurgical processes, but it also contains some level of radionuclides. Relatively high neutralisation conditions (120 - 150 °C, P_{CO2} = 30 bar) did not change the initial concentrations of radionuclides, and they remained similar to the original sample, i.e. < 500 Bq kg^{-1}. However, the recovery of Fe by smelting BR led to a radionuclide enrichment in the slag of about 1.5 times compared to the initial concentration, without exceeding 800 Bq kg^{-1}. Further processing of the BR slag by HPAL can cause accumulation of radionuclides in the remaining solid residue, depending on the smelting conditions (flux utilised) and on the type of mineral acid used in the subsequent leaching step. Thus, a concentration of ^{228}Th > 1000 Bq kg^{-1} was only observed in the solid residues remaining from the leaching experiment in which the slag produced with an excess of CaO (no addition of SiO_2 as flux) was leached with HCl. The concentration of radionuclides in the corresponding leach liquors was not higher than 100 Bq L^{-1}, but it is difficult to conclude whether the mineral acids used in this research can have a preferential effect on the dissolution of radionuclides. The analytical model demonstrated that under the experimental conditions considered in this research, the solid residues and leach liquors are unlikely to exceed annual doses of 1 mSv, which is set as limiting exposure criterion for public in the EU BSS. The same conclusion holds even if the experimental conditions are upscaled to industrial levels. The described radiological exposure assessment implies that the natural radionuclides present in the studied BR are unlikely to be radiologically hazardous to workers; radiological properties of the studied material are not predicted to be a limiting factor during industrial operation. However, it should be noted that these conclusions are valid for one specific BR studied in

this work, as the chemical and radiological properties can vary considerably based on batch and geographic origin.

Although several technologies have been reported to recover metals from BR, few studies have addressed the occurrence of radionuclides in the process streams. As highlighted in this work, the radiological exposure assessment for the specific BR studied yielded the conclusion that radiological properties would not be a limiting factor for industrial processes using this specific BR; however many previously reported BR-related technologies have not benefited from such an assessment. A critical ongoing and future need is to ensure safety and regulatory compliance; hence, it is highly important that the presence of natural radionuclides should be considered in process technologies for metal recovery from BR.

Future research may address approaches to facilitate this goal in an accurate yet unobtrusive way. Some efforts in this regard have been reported, including a framework for including enhanced exposure to naturally occurring radioactive materials (NORM) in Life Cycle Assessment (Joyce et al., 2017) and development of relevant impact assessments (Goronovski et al., 2018).

Supplementary Material

Table S1: Isotope concentrations in raw slag subjected to fast cooling (Bq kg^{-1})

Isotope series	Isotope	Slag I	Slag II	Slag III
^{238}U	^{226}Ra	300±14	262±9	280±13
^{232}Th	^{228}Ra	675±42	629±35	666±40
	^{228}Th	697±17	624±37	691±41
^{40}K		101±98	108±43	<206

Table S2: Isotope concentrations in raw slag subjected to slow cooling (Bq kg^{-1})

Isotope series	Isotope	Slag I	Slag II	Slag III
^{238}U	^{226}Ra	313±15	305±14	276±16
^{232}Th	^{228}Ra	713±44	642±40	604±42
	^{228}Th	702±42	639±	622±39
^{40}K		<236	<232	126±113

Table S3: Modeled potential annual exposure from materials (mSv year^{-1})

Fast cooling	Slag I	Slag II	Slag III
	0.39	0.35	0.39
Slow cooling	Slag I	Slag II	Slag III
	0.41	0.38	0.36

Table S4: Solid residues, produced after HPAL with HCl acid (Bq kg^{-1})

Isotope series	Isotope	Fast cooling			Slow cooling			BR
		Slag I	Slag II	Slag III	Slag I	Slag II	Slag III	
^{238}U	^{226}Ra	46±14	144±9	N.d.	122±9	161±62	60±8	127±10
^{232}Th	^{228}Ra	<155	321±14		294±13	358±10	<96	290±16
	^{228}Th	1645±36	491±14		1250±26	512±11	639±15	327±12
^{40}K		<508	<323		<336	<194	<309	<387

Table S5: Solid residues, produced after HPAL with H_2SO_4 acid (Bq kg^{-1})

Isotope series	Isotope	Fast cooling			Slow cooling			BR
		Slag I	Slag II	Slag III	Slag I	Slag II	Slag III	
^{238}U	^{226}Ra	229±11	218±12	N.d.	213±8	N.d.	205±7	137±7
^{232}Th	^{228}Ra	568±19	457±19		447±18		484±12	277±11
	^{228}Th	501±14	399±14		319±10		419±10	266±9
^{40}K		<370	<409		<501		<199	<254

Table S6: Pregnant leachate solution, produced after HPAL with HCl acid (Bq L^{-1})

Isotope series	Isotope	Fast cooling			Slow cooling			BR
		Slag I	Slag II	Slag III	Slag I	Slag II	Slag III	
^{238}U	^{226}Ra	<4	<6	29±2	25±2	28±2	N.d.	9±1
^{232}Th	^{228}Ra	<12	<16	73±6	<24	69±49		<18
	^{228}Th	2±1	19±2	15±2	13±2	29±2		39±1
^{40}K		<52	<65	<87	<69	<62		<71

Table S7: Pregnant leachate solution, produced after HPAL with H_2SO_4 acid (Bq kg^{-1})

Isotope series	Isotope	Fast cooling			Slow cooling			BR
		Slag I	Slag II	Slag III	Slag I	Slag II	Slag III	
^{238}U	^{226}Ra	<4	<4	N.d.	6±1	<	4±1	6±1
^{232}Th	^{228}Ra	<11	14±1		<13	<12	<13	<15
	^{228}Th	14±1	<3		28±2	20±2	16±2	18±2

^{40}K	<49	<54	59	<52	<59	<62

Table S8: Modeled potential annual exposure from materials (mSv year^{-1})

Product	Leaching reagent	Fast cooling			Slow cooling			BR
		Slag I	Slag II	Slag III	Slag I	Slag II	Slag III	
Solid	HCl	0.73	0.26	N.d.	0.58	0.27	0.30	0.19
	H_2SO_4	0.30	0.25		0.22	N.d.	0.25	0.16
Liquid	HCl	$6.5 \cdot 10^{-3}$	$9.6 \cdot 10^{-2}$	$3.6 \cdot 10^{-3}$	$1.7 \cdot 10^{-2}$	$3.3 \cdot 10^{-2}$	N.d.	$1.8 \cdot 10^{-2}$
	H_2SO_4	$4.7 \cdot 10^{-3}$	$4.7 \cdot 10^{-3}$	N.d.	$8.4 \cdot 10^{-3}$	$6.3 \cdot 10^{-3}$	$5.4 \cdot 10^{-3}$	$6.1 \cdot 10^{-3}$

Acknowledgements

The research leading to these results has received funding from the European Union's Horizon 2020 research and innovation programme (H2020/2014–2019) under Grant Agreement No. 636876 (MSCA-ETN REDMUD). This publication reflects only the authors' view, exempting the European Union from any liability. Project website: http://www.etn.redmud.org. The authors thank Mytilineos S.A. - Aluminium of Greece for providing the BR samples.

References

Akinci, A., Artir, R., 2008. Characterization of trace elements and radionuclides and their risk assessment in red mud. Mater. Charact. 59, 417–421. https://doi.org/10.1016/j.matchar.2007.02.008

Barakos, G., Mischo, H., Gutzmer, J., 2014. Assessments of boundary conditions and requirements for Rare Earth Underground Mining due to presence of NORMs. Proceedings of the 1st Conference on European Rare Earth Resources 2014 (ERES 2014). Milos, Greece, 4-7 September 2014, pp. 133-139.

Borra, C.R., Pontikes, Y., Binnemans, K., Van Gerven, T., 2015. Leaching of rare earths from bauxite residue (red mud). Miner. Eng. 76, 20–27. https://doi.org/10.1016/j.mineng.2015.01.005

Borra, C.R., Blanpain, B., Pontikes, Y., Binnemans, K., Van Gerven, T., 2016. Recovery of rare earths and other valuable metals from bauxite residue (red mud): a review. J. Sustain. Met. 2, 365–386. https://doi.org/10.1007/s40831-016-0068-2

Cooper, M.B., 2005. Naturally Occurring Radioactive Materials (NORM) in Australian Industries - Review of Current Inventories and Future Generation, EnviroRad Services Pty. Ltd.

Cuccia, V., Oliveira, A.H. de, Rocha, Z., 2011. Radionuclides in Bayer Process Residues: Previous Analysis for Radiological Protection, in: International Nuclear Atlantic Conference - INAC.

Belo Horizonte.

European Commission, 1999. Radiological Protection Principles concerning the Natural Radioactivity of Building Materials.

European Parliament, 2014. Council Directive 2013/59/Euratom of 5 December 2013 laying down basic safety standards for protection against the dangers arising from exposure to ionising radiation, and repealing Directives 89/618/Euratom, 90/641/Euratom, 96/29/Euratom, 97/43/Euratom, Off J Eur Commun L13 1–73.

Evans, K., 2016. The History, Challenges, and New Developments in the Management and Use of Bauxite Residue. J. Sustain. Met. 2, 316–331. https://doi.org/10.1007/s40831-016-0060-x

Gamaletsos, P., Godelitsas, A., Mertzimekis, T.J., Göttlicher, J., Steininger, R., Xanthos, S., Berndt, J., Klemme, S., Kuzmin, A., Bárdossy, G., 2011. Thorium partitioning in Greek industrial bauxite investigated by synchrotron radiation and laser-ablation techniques. Nucl. Instruments Methods Phys. Res. Sect. B Beam Interact. with Mater. Atoms 269, 3067–3073. https://doi.org/10.1016/j.nimb.2011.04.061

Gamaletsos, P.N., Godelitsas, A., Kasama, T., Church, N.S., Douvalis, A.P., Göttlicher, J., Steininger, R., Boubnov, A., Pontikes, Y., Tzamos, E., Bakas, T., Filippidis, A., 2016a. Nano-mineralogy and -geochemistry of high-grade diasporic karst-type bauxite from Parnassos-Ghiona mines, Greece. Ore Geol. Rev. 84, 228–244. https://doi.org/10.1016/j.oregeorev.2016.11.009

Gamaletsos, P.N., Godelitsas, A., Kasama, T., Kuzmin, A., Lagos, M., Mertzimekis, T.J., Göttlicher, J., Steininger, R., Xanthos, S., Pontikes, Y., Angelopoulos, G.N., Zarkadas, C., Komelkov, A., Tzamos, E., Filippidis, A., 2016. The role of nano-perovskite in the negligible thorium release in seawater from Greek bauxite residue (red mud). Sci. Rep. 6, 21737. https://doi.org/10.1038/srep21737

Gupta, C.K., Krishnamurthy, N., 2005. Extractive Metallurgy of Rare Earths, CRC Press, Boca Raton, Florida. https://doi.org/10.1007/s13398-014-0173-7.2

Goronovski, A., Joyce, P.J., Björklund, A., Finnveden, G., Tkaczyk, A.H., 2018. Impact assessment of enhanced exposure from Naturally Occurring Radioactive Materials (NORM) within LCA. Journal of Cleaner Production 172, 2824–2839. https://doi.org/10.1016/j.jclepro.2017.11.131

Goronovski, A., Tkaczyk, A.H., 2019. Radiological assessment of the bauxite residue valorization chain. J. Radioanal. Nucl. Chem 321, 955–963 (2019). https://doi.org/10.1007/s10967-019-06676-6

Goronovski, A., Vind, J., Vassiliadou, V., Panias, D., Tkaczyk, A.H., 2019. Radiological assessment of the Bayer process. Miner. Eng. 137, 250–258. https://doi.org/10.1016/j.mineng.2019.04.016

Gu, H., Wang, N., Yang, Y., Zhao, C., Cui, S., 2017. Features of distribution of uranium and thorium in red mud. Physicochem. Probl. Miner. Process. 53, 110–120.

Hegedűs, M., Tóth-Bodrogi, E., Jónás, J., Somlai, J., Kovács, T., 2018. Mobility of 232Th and 210Po in red mud. J. Environ. Radioact. 184–185, 71–76. https://doi.org/10.1016/j.jenvrad.2018.01.012

IAEA, 2010. Analytical Methodology for the Determination of Radium Isotopes in Environmental Samples, IAEA Analytical Quality in Nuclear Applications Series. Vienna.

IAEA, 2003. Extent of Environmental Contamination by Naturally Occurring Radioactive Material (NORM) and Technological Options for Mitigation, La Prensa medica mexicana. Vienna.

International Aluminium Institute, 2015. Bauxite Residue Management : Best Practice. London.

Joyce, P.J., Goronovski, A., Tkaczyk, A.H., Björklund, A., 2017. A framework for including enhanced exposure to naturally occurring radioactive materials (NORM) in LCA. Int J Life Cycle Assess 22, 1078–1095. https://doi.org/10.1007/s11367-016-1218-2

Markkanen, M., 1995. Radiation Dose Assessments for Materials with Elevated Natural

Radioactivity, Nuclear Safety.

Narayanan, R.P., Ma, L.-C., Kazantzis, N.K., Emmert, M.H., 2018. Cost Analysis as a Tool for the Development of Sc Recovery Processes from Bauxite Residue (Red Mud). ACS Sustain. Chem. Eng. 6. https://doi.org/10.1021/acssuschemeng.8b00107

Nuccetelli, C., Pontikes, Y., Leonardi, F., Trevisi, R., 2015. New perspectives and issues arising from the introduction of (NORM) residues in building materials: A critical assessment on the radiological behaviour. Constr. Build. Mater. 82, 323–331. https://doi.org/10.1016/j.conbuildmat.2015.01.069

Pontikes, Y., Angelopoulos, G.N., 2013. Bauxite residue in cement and cementitious applications: Current status and a possible way forward. Resour. Conserv. Recycl. 73, 53–63. https://doi.org/10.1016/j.resconrec.2013.01.005

Rivera, R.M., Ounoughene, G., Borra, C.R., Binnemans, K., Van Gerven, T., 2017a. Neutralisation of bauxite residue by carbon dioxide prior to acidic leaching for metal recovery. Miner. Eng. 112, 92–102. https://doi.org/10.1016/j.mineng.2017.07.011

Rivera, R.M., Ounoughene, G., Malfliet, A., Vind, J., Panias, D., Vassiliadou, V., Binnemans, K., Van Gerven, T., 2019a. A Study of the Occurrence of Selected Rare-Earth Elements in Neutralized–Leached Bauxite Residue and Comparison with Untreated Bauxite Residue. J. Sustain. Metall. 5, 57–68. https://doi.org/10.1007/s40831-018-0206-0

Rivera, R.M., Ulenaers, B., Ounoughene, G., Binnemans, K., 2017b. Behaviour of Silica during Metal Recovery from Bauxite Residue by Acidic Leaching, in: 35th International ICSOBA Conference, Hamburg, Germany, 2 – 5 October, 2017. pp. 547–556.

Rivera, R.M., Xakalashe, B., Ounoughene, G., Binnemans, K., Friedrich, B., Van Gerven, T., 2019b. Selective rare earth element extraction using high-pressure acid leaching of slags arising from the smelting of bauxite residue. Hydrometallurgy 184, 162–174. https://doi.org/10.1016/j.hydromet.2019.01.005

Rubinos, D. a, Barral, M.T., 2013. Fractionation and mobility of metals in bauxite red mud. Environ. Sci. Pollut. Res. Int. 20, 7787–802. https://doi.org/10.1007/s11356-013-1477-4

Samouhos, M., Taxiarchou, M., Tsakiridis, P.E., Potiriadis, K., 2013. Greek “red mud” residue: A study of microwave reductive roasting followed by magnetic separation for a metallic iron recovery process. J. Hazard. Mater. 254–255, 193–205. https://doi.org/10.1016/j.jhazmat.2013.03.059

Somlai, J., Jobbágy, V., Kovács, J., Tarján, S., Kovács, T., 2008. Radiological aspects of the usability of red mud as building material additive. J. Hazard. Mater. 150, 541–545. https://doi.org/10.1016/j.jhazmat.2007.05.004

UNSCEAR, 2000. Sources and Effects of Ionizing Radiation, Report to the General Assembly,with scientific annexes. https://doi.org/10.1097/00004032-199907000-00007

Vidmar, T., 2005. EFFTRAN — A Monte Carlo efficiency transfer code for gamma-ray spectrometry. Nucl. Instruments Methods Phys. Res. A 550, 603–608. https://doi.org/10.1016/j.nima.2005.05.055

Vind, J., Malfliet, A., Blanpain, B., Tsakiridis, P., Tkaczyk, A., Vassiliadou, V., Panias, D., 2018. Rare Earth Element Phases in Bauxite Residue. Minerals 8, 77. https://doi.org/10.3390/min8020077